A New Multiharmonic Loading Method for Large-Signal Microwave and Millimeter-Wave Transistor Characterization

Fadhel M. Ghannouchi, *Member, IEEE*, Robert Larose, and Renato G. Bosisio, *Senior Member, IEEE*

Abstract—**A new multiharmonic loading method for nonlinear microwave and millimeter-wave transistor characterization using six-port techniques is presented. The system allows independent load tuning of an excitation signal and its harmonics. Load-pull measurements on a MESFET have been performed at the fundamental frequency, f_0, and at the second $(2f_0)$ and third $(3f_0)$ harmonics. The results highlight the importance of such measurement in designing and modeling nonlinear devices and circuits. The experimental results were found to be directly applicable for optimizing efficiency and output power in high-power MESFET amplifiers and MESFET frequency multipliers.**

TABLE I
NINE POSSIBLE TESTS: HARMONIC POWER CONTOUR $P(nf_0)$ VERSUS HARMONIC COMPLEX PLANE $\Gamma(nf_0)$ (ACTUAL TESTS PERFORMED DENOTED BY "x")

Harmonic Complex Plane	Harmonic Power Contour		
	$P_L(f_0)$	$P_L(2f_0)$	$P_L(3f_0)$
$\Gamma_L(f_0)$	x	x	
$\Gamma_L(2f_0)$		x	
$\Gamma_L(3f_0)$	x		x

I. INTRODUCTION

THE trend toward better large-signal modeling of active devices triggers the need for simple and pertinent nonlinear measurements and characterization. Methods such as load-pull using automatic tuners [1], active load-pull [2], harmonic load-pull [3], and measurement of the amplitude and phase of harmonics [4] provide a good insight into nonlinear devices and circuits. High-power microwave and millimeter-wave transistor characterization (load-pull measurement) is not always easily done when using directional couplers, automatic tuners, and automatic network analyzers (ANA's). Numerical corrections arising from the nonideal behavior of directional couplers are often needed in power flow and impedance measurements [5], [6]. On the other hand, MESFET frequency multipliers can exhibit a conversion gain and good efficiency for multiplication factors of 2×, 3×, and 4× [7]. Output power and efficiency can be maximized by optimizing the harmonic loading of MESFETs used in designing power amplifiers and frequency multipliers. In order to use a nonlinear CAD simulator, one has to have a good library of nonlinear models for the large number of available packages, chips, and transistors. Unfortunately, the modeling is often done only for a few devices and mainly at the chip level.

Manuscript received September 24, 1990; revised January 29, 1991.
The authors are with the Department of Electrical Engineering, Ecole Polytechnique de Montréal, C. P. 6079, Succursale A, Montréal, Québec, Canada H3C 3A7.
IEEE Log Number 9144290.

This paper presents an experimental procedure for characterizing a microwave and millimeter-wave transistor under different harmonic loads using an active multiharmonic load-pull method and six-port techniques. This method is an extension of the well-known active load-pull technique [2], and the number of harmonics considered is not limited by the bandwidth of circulators used in other systems [3]. The setup consists of a wide-band dual six-port network analyzer [8] with frequency selective power detectors used in an active load-pull tuning configuration [9]. The originality of this method lies in its use of the linearity of the six-port junction to handle signals at different frequencies simultaneously. This property leads to the possibility of independent load tuning at each harmonic, including the fundamental (f_0). This paper illustrates a new characterization system to investigate harmonic load tuning using second and third harmonics of the excitation signal. Constant output power $P(f_0)$ contours were obtained in a variable complex $\Gamma_L(f_0)$ plane for chosen values of $\Gamma_L(2f_0)$ and $\Gamma_L(3f_0)$. Similarly, constant power contours for $P(2f_0)$ were obtained in a variable complex $\Gamma_L(f_0)$ plane with chosen and fixed values of $\Gamma_L(2f_0)$ and $\Gamma_L(3f_0)$. In addition, two other test conditions of the total nine possible test conditions for the fundamental, second, and third harmonics are presented. Fixed values of Γ_L in the nontest harmonic plane were chosen and kept constant during the measurements, in order to satisfy a given design criterion (e.g. minimum or maximum power level at a given harmonic). More

0018-9480/91/0600-0986$01.00 ©1991 IEEE

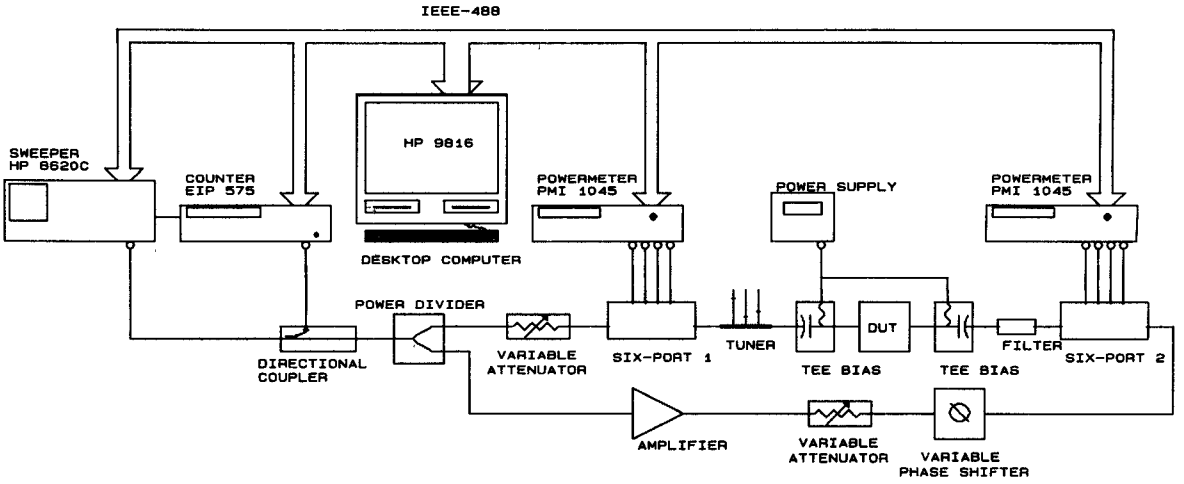

Fig. 1. Experimental block diagram of single-frequency load-pull characterization setup.

TABLE II
MECHANICAL TUNER* INSERTION LOSS VARIATION VERSUS STUB POSITION ($f = 3.5$ GHz)

Tuner Input Reflection Coefficient	Input Power P_{in} (dBm)	Output Power P_{out} (dBm)	Insertion Loss (dB)
Position 1 $\Gamma_L = 0.39/45°$	12.13	11.79	0.34
Position 2 $\Gamma_L = 0.72/-17°$	8.89	6.60	2.29
Position 3 $\Gamma_L = 0.79/136°$	8.35	−6.88	15.23
Position 4 $\Gamma_L = 0.10/-152°$	12.95	12.13	0.82

*Tuner: Maury Microwave Model 1819C.

harmonics could be used by this test method by upgrading the measurement system. Table I indicates the five tests presented in this paper.

Experimental results were found to be directly applicable to frequency multipliers and high-power amplifier design. It was found also that MESFET harmonic loading has little effect on harmonic generation processes. However, harmonic impedances are important in determining the harmonic power coupled to the output circuit. In addition, it was experimentally demonstrated for the first time that the efficiency of MESFET power amplifiers can be optimized by tuning the third-harmonic impedance at fixed fundamental and second-harmonic impedances for a given output power. In the case of the NEC 71083 MESFET used as a class AB amplifier, its efficiency can be improved by 10% by tuning the third harmonic load.

II. Active Tuning Method Using Six-Port Techniques

The experimental setup for active load-pull measurement is similar to the setup used with dual six-port network analyzers (see Fig. 1). The feasibility of a dual six-port network analyzer as a load-pull system in a single-frequency active load tuning configuration has been presented in a previous paper [9]. Each six-port junction (SP1 and SP2) was calibrated for impedance and power flow measurements at the operating frequency [6], [10]. The calibration of SP1 incorporates a mechanical tuner and a bias tee; the calibration of SP2 incorporates a bias tee and a filter (see Fig. 1.). A variable phase shifter and a programmable attenuator are inserted into the output branch to set the output impedance, and a second attenuator is added into the input branch to maintain a constant level of power absorbed by the transistor. A Boonton 4300 with an appropriate power sensor (Boonton model 51013) is used as an external power meter to perform the power calibration [6]. The transistor under test is placed in an appropriate fixture and the de-embedding is done using the TRL method [11]. The measurement sequence begins with the adjustment of P_{in}, the phase shifter is then positioned to the desired phase, ϕ_L, and finally a scanning of the magnitude of Γ_L is performed with the programmable attenuator. With a programmable phase shifter, the complete scanning of the Smith chart can be fully automated without complex algorithms since the attenuator introduces a quasi-constant phase shift over a large dynamic range.

Experimental measurements were performed on a MESFET (NEC 71083) operated in class AB made with an input power of 4 dBm at 3.5 GHz ($V_{ds} = 3$ V, $I_{ds} = 10$ mA, $V_{gs} = -0.24$ V). The measurements include P_{in} (power input to the transistor), P_L (power dissipated in the load impedance), Γ_{in} (large-signal input reflection coefficient), Γ_L (load reflection coefficient presented to the transistor), I_{ds} (dc drain current), and V_{gs} (dc gate-to-source voltage). The input matching network is a mechanical tuner with fixed stub positions to match the source

TABLE III
COMPARISON BETWEEN ACTIVE TUNING METHOD AND MECHANICAL TUNING METHOD FOR LOAD-PULL MEASUREMENTS ON NEC 71083 MESFET (P_{in} = 4 dBm, f = 3.5 GHz, V_{ds} = 3 V, I_{ds} = 10 mA, V_{gs} = −0.24 V)

	$\Gamma_L = 0.39\angle 45°$			$\Gamma_L = 0.72\angle -17°$			$\Gamma_L = 0.79\angle 136°$			$\Gamma_L = 0.10\angle -152°$		
	P_L (dBm)	I_{ds} (mA)	η_a (%)	P_L (dBm)	I_{ds} (mA)	η_a (%)	P_L (dBm)	I_{ds} (mA)	η_a (%)	P_L (dBm)	I_{ds} (mA)	η_a (%)
Active Tuning Method	15.79	21.06	56.1	12.35	23.72	20.6	6.75	28.12	2.6	13.20	25.81	23.7
Mechanical Tuning Method	15.49	20.61	53.2	12.38	23.50	21.0	6.98	27.94	3.0	13.31	25.51	24.7

impedance to the input impedance of the test transistor for the input driving power level of 4 dBm (see Fig. 1).

To check the accuracy of the method, a mechanical tuner (Maury model 1819C) is first used to simulate four different loads. For each stub position corresponding to a given impedance, the tuner is disconnected after the load-pull measurements in order to evaluate its impedance and insertion loss. Table II summarizes the results and highlights the large variations in the insertion losses with the positions of the tuner stubs. The same four impedances are presented to the transistor under test using the active load-pull configuration. The same filter is placed just after the transistor to maintain the same harmonic loads for both mechanical and active tuner configurations. Table III regroups both measurements, including input and output power, dc drain current I_{ds}, and power-added efficiency η_a calculated using the following equation:

$$\eta_a = 100\% \frac{P_L(\text{mW}) - P_{in}(\text{mW})}{P_{dc}(\text{mW})} \% \tag{1}$$

where

$$P_{dc} = I_{ds} V_{ds}. \tag{2}$$

The two methods agree well considering the number of manipulations needed for the characterization using the mechanical tuner (see Table III).

III. Multisignal Impedance and Power Flow Measurements Using Six-Port Techniques

The principal component of the system is a wide-band six-port junction. Because the junction is passive and linear, signals at n multiple frequencies of f_0 can be present in the six-port without interfering with each other. Consequently, with appropriate sampling and filtering circuits at detection level, one can isolate harmonics and measure them independently. In such a case the multisignal six-port reflectometer is equivalent to n single-frequency six-port reflectometers. The basic equations describing the six-port reflectometer [8] and [10] can be extended for the nth harmonic of a fundamental signal, f_0, as follows:

$$P_i(nf_0) = A_i(nf_0)\left|\Gamma(nf_0) - Q_i(nf_0)\right|^2 \left|b(nf_0)\right|^2 \tag{3}$$

with $i = 3,4,5,6$ and $n = 1,2,3,\cdots,N$. Here $P_i(nf_0)$ is the power reading of the nth harmonic at port i; $Q_i(nf_0)$ and $A_i(nf_0)$ are calibration parameters of the nth-harmonic equivalent six-port reflectometer; $b(nf_0)$ is the incident normalized voltage at the DUT at the nth harmonic; and $\Gamma(nf_0)$ is the reflection coefficient measured at the nth harmonic.

Calibration of each equivalent six-port is done independently using a standard method [6]. In addition, power flow measurement with the six-port junction [9] can also be transposed to each harmonic as follows:

$$P_f(nf_0) = \frac{K(nf_0) P_3(nf_0)}{\left|1 + C(nf_0)\Gamma(nf_0)\right|^2}, \qquad n = 1,2,3,\cdots,N. \tag{4}$$

Here $C(nf_0)$ is the de-embedding calibration parameters obtained by six-port error box calibration at the nth harmonic; $K(nf_0)$ is a scalar parameter which characterizes the nth six-port reflectometer associated with the nth harmonic and is obtained by power calibration [9]; and $P_3(nf_0)$ is the power reading at port 3 associated with the nth equivalent six-port reflectometer.

From the values of $\Gamma(nf_0)$ and $P(nf_0)$ one can calculate the impedance of the DUT $Z(nf_0)$ and the power absorbed by that DUT, $P_a(nf_0)$, as follows:

$$Z(nf_0) = Z_0 \frac{1 + \Gamma(nf_0)}{1 - \Gamma(nf_0)} \tag{5}$$

$$P_a(nf_0) = Pf(nf_0)\left(1 - \left|\Gamma(nf_0)\right|^2\right) \tag{6}$$

with $n = 1,2,3,\cdots,N$.

The original multisignal operation of the six-port reflectometer as detailed above can be advantageously used in the nonlinear characterization of microwave and millimeter-wave solid-state devices such as MESFET's, HEMT's, and Gunn diodes.

IV. Multiharmonic Load-Pull System

The experimental setup for multiharmonic active load-pull measurements is shown in Fig. 2. The six-port reflectometers SP1 and SP2 are calibrated independently for impedance and power-flow measurements over a 2–12 GHz frequency band [6]. Impedance measurements and power-flow measurements at each frequency can be performed using appropriate dividing/filtering circuits before power detection, as shown in the last section. The input excitation frequency signal, f_0, the second harmonic, $2f_0$, and the third harmonic, $3f_0$, are injected

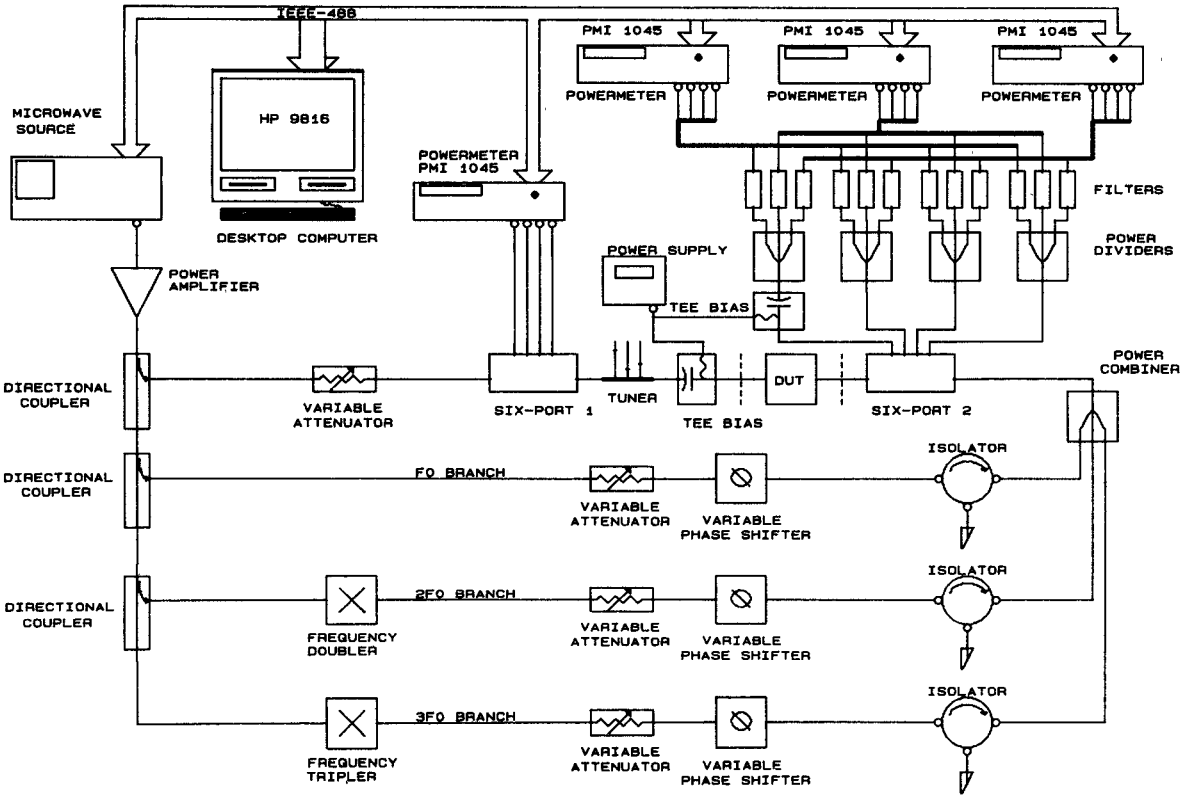

Fig. 2. Experimental block diagram of multiharmonic load-pull system.

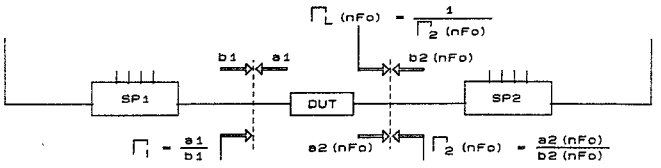

Fig. 3. Multiharmonic active load-pull tuning configuration using six-port network analyzer.

simultaneously at the input of the second six-port junction, SP2, by means of a three-way power combiner as shown in Fig. 2.

In the case of active load-pull measurements with a six-port network analyzer [9], evaluation of the large-signal input impedance, Γ_{in}, of the transistor and of the power delivered to the device, P_{in}, is directly available by measurements at the input six-port (SP1). The active harmonic loads presented to the transistor under test and the power delivered to these loads can be deduced from measurements using the following relations (see Fig. 3):

$$\Gamma_L(nf_0) = \frac{1}{\Gamma_2(nf_0)} \tag{7}$$

$$Z_L(nf_0) = Z_0 \frac{1+\Gamma_L(nf_0)}{1-\Gamma_L(nf_0)} = Z_0 \frac{\Gamma_2(nf_0)+1}{\Gamma_2(nf_0)-1} \tag{8}$$

and

$$P_L(nf_0) = P_f(nf_0)\left(\left|\Gamma_2(nf_0)\right|^2 - 1\right) \tag{9}$$

with $n = 1$, 2, and 3. Here $P_f(nf_0)$ and $\Gamma_2(nf_0)$ are actual measurements by the output equivalent six-port (SP2) at the nth harmonic.

A variable attenuator and variable phase shifter are inserted in the fundamental branch (between the three-way power combiner and the directional coupler, DC1) to change the simulated load impedance seen by the transistor at f_0. The second (third) harmonic branch includes a frequency doubler (tripler) and amplitude and phase controllers as required to synthesize the desired second (third) harmonic impedance to be seen by the microwave transistor operating in a nonlinear mode. Three narrow-band isolators (one in each branch) are used to facilitate independent harmonic impedance tuning. At each detection port of SP2, the multifrequency signal is split into three parts using a wide-band three-way unequal power divider; three band-pass filters, centered respectively at f_0, $2f_0$, and $3f_0$, are used to selectively recover the signals at f_0, at $2f_0$, and at $3f_0$ from the multifrequency signal. The outputs of these band-pass filters are connected to three four-channel power meters as shown in Fig. 2. A high-power amplifier is inserted at the output of the microwave generator in order to a) saturate the MESFET (NEC 71083), b) provide enough power for the frequency doubler and frequency tripler, and c) allow the simulation of any passive load at f_0 at the output of the test transistor. A frequency doubler and a frequency tripler should provide sufficient harmonic power to permit the simulation of any passive load at each harmonic which might be seen by the MESFET. The bandwidth of the branch phase/amplitude controllers is lower than the

required six-port reflectometer bandwidth. The gate of the MESFET is biased by means of a T junction placed before the test fixture. However, the T junction used to bias the drain is placed at the output of port 3 of SP2; this is because inside SP2 a dc connection is available between port 3 and its measuring port. The extension of this measurement system to investigate higher harmonics is straightforward by adding more harmonic branches and by using appropriate dividing/filtering circuits before power detection.

In practical situations s_{12} of the MESFET under test is small compared with s_{21}. Moreover, because of losses and attenuation between the output of the MESFET and the four detectors of SP1, no harmonic signals reach the four detectors of SP1.

V. Experimental Large-Signal Characterization of a MESFET

Experimental measurements were performed on an NEC 71083 MESFET operated in class AB made at 2.4 GHz and 3.6 GHz. Polarization voltages and current are as follows: $V_{ds} = 3$ V, $I_{ds} = 10$ mA, and $V_{gs} = -.24$ V. The measurements include:

- $P_{in}(f_0)$: power input to the test transistor obtained by SP1;
- $P_L(f_0)$: power delivered to load impedance $Z_L(f_0)$, obtained by SP2;
- $P_L(nf_0)$: harmonic power delivered to the harmonic load impedance $Z_L(nf_0)$, obtained by SP2;
- $\Gamma_{in}(f_0)$: large-signal input reflection coefficient, obtained by SP1;
- $\Gamma_L(f_0)$: reflection coefficient associated with the load seen by the transistor $Z_L(f_0)$, obtained by SP2;
- $\Gamma_L(nf_0)$: reflection coefficient associated with the harmonic load seen by the transistor $Z_L(nf_0)$, obtained by SP2;
- I_{ds}: dc drain current measured by a millimeter;
- V_{gs}: dc gate voltage measured by a voltmeter;
- V_{ds}: dc drain voltage measured by a voltmeter.

In this paper, only the second- and third-harmonic loadings are investigated ($n = 2$ and 3). Fig. 4 shows conventional constant-power contours $P_L(f_0)$ in the $\Gamma_L(f_0)$ plane where the values of $\Gamma_L(2f_0)$ and $\Gamma_L(3f_0)$ were set at $0.22\angle 53°$ and $0.52\angle 113°$ respectively. The power-added efficiency (η_a) contours (Fig. 4) are obtained using (1). Fig. 5 shows constant-power contours $P(2f_0)$ in the $\Gamma_L(f_0)$ plane. It is seen that the optimum load for frequency doubling lies in the region $\Gamma_L = 0.9\angle 70°$ (area of maximum power level at $2f_0$), and the optimum load as an amplifier lies in the region $\Gamma_L = 0.5\angle 20°$ (area of minimum power at $2f_0$). It is also seen that the load for maximum efficiency given by Fig. 5 corresponds to a minimum power at the second harmonic (Fig. 5) for the given bias test conditions. Fig. 6 shows constant-power contours $P_L(2f_0)$ in the $\Gamma_L(2f_0)$ plane for fixed value of

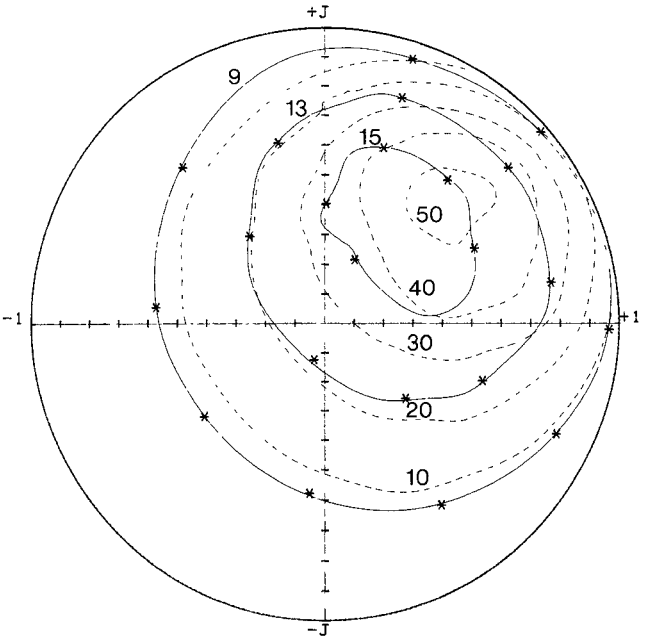

Fig. 4. Constant power contours $P_L(f_0)$ expressed in dBm in the complex $\Gamma_L(f_0)$ plane (——— line type, * experimental measured points). Power added efficiency contours expressed as a percentage in the complex $\Gamma_L(f_0)$ plane (– – – line type), ($f_0 = 3.6$ GHz; $P_{in} = 4$ dBm). Transistor NEC 71083 $V_{ds} = 3$ V, $I_{ds} = 10$ mA, $V_{gs} = -0.24$ V.

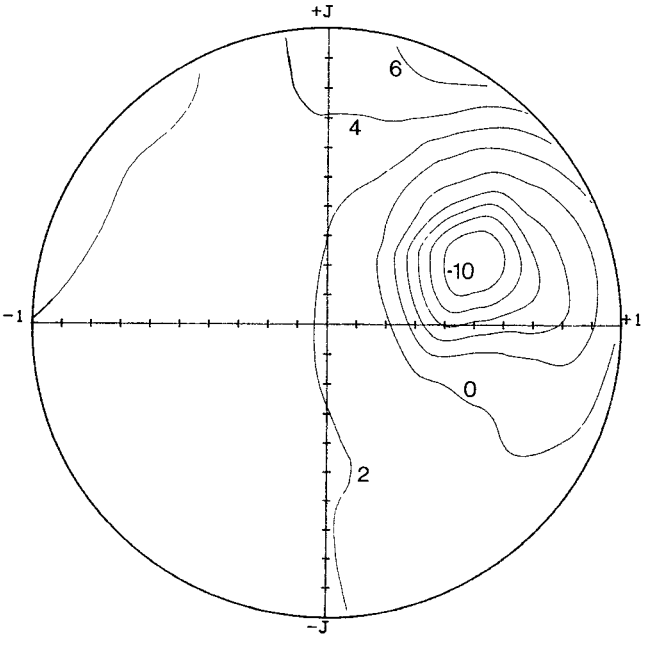

Fig. 5. Constant power contours $P_L(2f_0)$ expressed in dBm in the complex $\Gamma_L(f_0)$ plane ($f_0 = 3.6$ GHz; $P_{in} = 4$ dBm). Transistor NEC 71083 $V_{ds} = 3$ V, $I_{ds} = 10$ mA, $V_{gs} = -0.24$ V.

$\Gamma_L(f_0)$ and $\Gamma_L(3f_0)$, respectively, set at $0.64\angle -29°$ and $0.52\angle 113°$. It is found that the maximum power level at the second harmonic lies in the region $0.5\angle -160°$. Fig. 7 shows constant-power contours $P_L(3f_0)$ in the $\Gamma_L(3f_0)$ plane for fixed values of $\Gamma_L(f_0)$ and $\Gamma_L(2f_0)$, respectively, set at $0.84\angle 29°$ and $0.21\angle -120°$. For all the above experimental results, the driving input power level is maintained at 4 dBm.

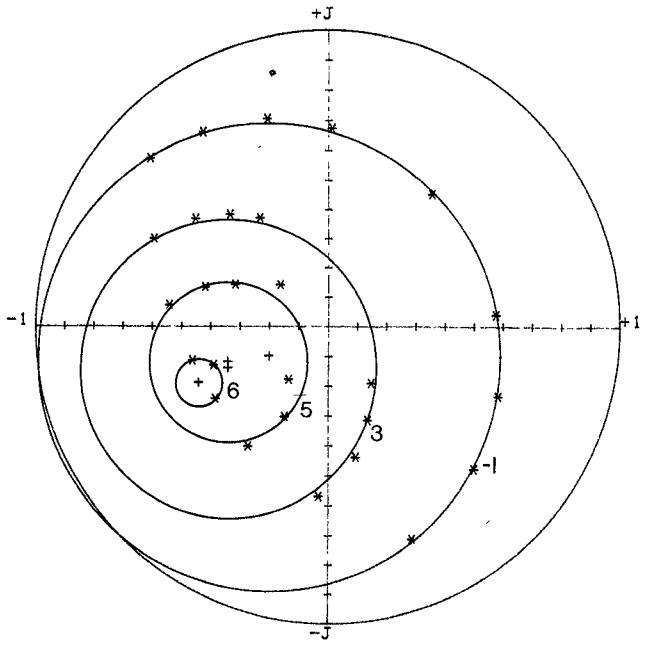

Fig. 6. Constant power contours $P(2f_0)$ expressed in dBm in the complex $\Gamma_L(f_0)$ plane, ($f_0 = 3.6$ GHz; $P_{in} = 4$ dBm). Transistor NEC 71083. $V_{ds} = 3$ V. $I_{ds} = 10$ mA, $V_{gs} = -0.24$ V. Asterisk denotes experimental measured points.

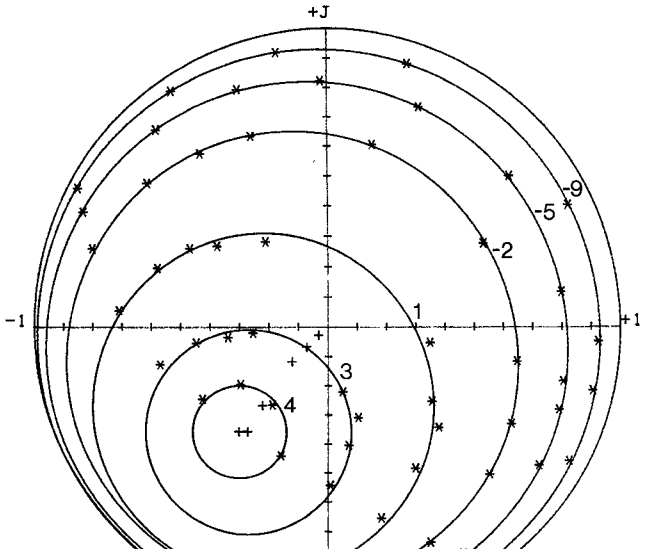

Fig. 7. Constant power contours $P_L(3f_0)$ expressed in dBm in the complex $\Gamma_L(3f_0)$ plane, ($f_0 = 2.4$ GHz; $P_{in} = 4$ dBm). Transistor NEC 71083 $V_{ds} = 3$ V, $I_{ds} = 10$ mA, $V_{gs} = -0.24$ V. Asterisk denotes experimental measured points.

To generate a specific constant-power or added efficiency contour, a data base over the entire Smith chart is obtained using data from experimental measurements (indicated by an asterisk in the figures) and an IMSL[1] interpolation routine (SURF). From such a data base any

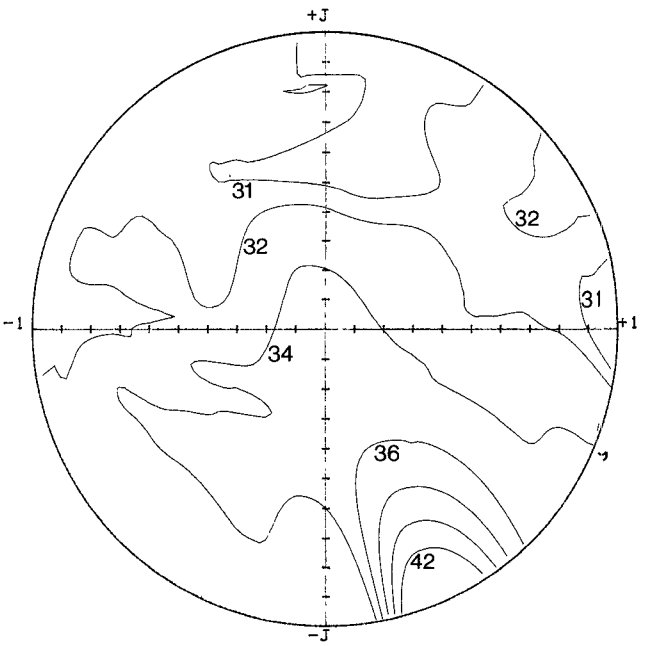

Fig. 8. Constant power added efficiency (percentage) contours in the complex $\Gamma_L(3f_0)$ ($f_0 = 2.4$ GHz; $P_{out} = 10$ dBm). Transistor NEC 71083. $V_{ds} = 3$ V, $I_{ds} = 10$ mA, $V_{gs} = -0.24$ V.

constant contours can be drawn using a second routine, BASIC/HP CONTOUR.[2]

To investigate the effect of the third-harmonic load on MESFET amplifier efficiency, output power was kept constant at 10 dBm as well as the fundamental load $\Gamma_L(f_0) = 0.84\angle +29°$ (area of maximum power level at $3f_0$) and the second-harmonic load $\Gamma_L(2f_0) = 0.21\angle -120°$, while the third harmonic was changed over the entire Smith chart. Fig. 8 shows the effect of third-harmonic loading on the efficiency of a MESFET amplifier. A 10% improvement in efficiency for a given output power can be obtained by optimizing the third-harmonic load. In aerospace applications, such an optimizing procedure can be very useful to minimize dc power requirements on high-power amplifiers operated at a given output power level.

The experimental points in Fig. 6 and 7 lie on quasi circles, indicating that harmonic loading has little effect on harmonic generation processes. However, harmonic impedances are important in determining the harmonic power coupled to the output circuit. Furthermore, harmonic impedances are also important in optimizing the efficiency of a MESFET working on an amplifier for a given and fixed output power. It is expected that MESFET multiharmonic load-pull characterization will permit an accurate determination of the most important nonlinear elements in MESFET models, such as c_{gs}, c_{ds}, and I_{ds} [12], by means of an appropriate nonlinear simulator (e.g. harmonic balance) and optimizing routines. The extension of this method to millimeter-wave transistor (e.g. HEMT) characterization is straightforward by using an appropri-

[1]IMSL Mathematical and Statistical Software Routines Library, IMSL vol. II, p. 516.

[2]BASIC 5.0 Graphics Techniques, Hewlett-Packard HP3000, Series 200, 300, No. 98613-90032, pp. 6–9.

ate wide-band dual six-port network analyzer [13], millimeter-wave amplitude and phase controllers, and millimeter-wave sampling and filtering circuits.

VI. Conclusion

A new multiharmonic load-pull method is presented in this paper. It is seen that this method can be useful for designing nonlinear circuits such as microwave and millimeter-wave power amplifiers or frequency doublers (triplers). It provides the quantitative data on fundamental and harmonic load impedances required to obtain a given performance from a MESFET operated in large-signal mode. This information can then be used to design the most suitable matching circuits for high-power amplifiers or MESFET frequency multipliers. Furthermore, it is expected that such multiharmonic characterization will prove very useful for MESFET nonlinear modeling. It is also expected that dual-gate MESFET's will be characterized using a multisignal loading method in order to design frequency mixers.

References

[1] J. M. Cusack *et al.*, "Automatic load contour mapping for microwave power transistors," *IEEE Trans. Microwave Theory Tech.*, vol. MTT-22, pp. 1146–1152, Dec. 1974.

[2] Y. Takayama, "A new load-pull characterization method for microwave power transistors," *IEEE MTT-S Int. Microwave Symp. Dig.*, June 1976, pp. 218–220.

[3] R. Stancliff and D. Poulin, "Harmonic load-pull," in *IEEE MTT-S Int. Microwave Symp. Dig.*, 1979, pp. 185–187.

[4] V. Lott, "A method for measuring magnitude and phase of harmonics generated in non-linear microwave two-ports," in *IEEE MTT-S Int. Microwave Symp. Dig.*, 1988, pp. 225–228.

[5] G. F. Engen, "The six-port reflectometer—An alternative network analyzer," *IEEE Trans. Microwave Theory Tech.*, vol. MTT-25, pp. 1075–1083, 1977.

[6] T. E. Hodgetts and G. J. Griffin, "A unified treatment of the six-port reflectometer calibration using the minimum of standards," Royal Signals and Radar Establishment, Report No. 83003, 1983.

[7] E. Camargo, R. Soares, R. A. Perichon, and M. Goloubkof, "Sources of non-linearity in GaAs MESFET frequency multipliers," in *IEEE MTT-S Int. Microwave Symp. Dig.*, 1983, pp. 343–345.

[8] G F. Engen, "The six-port reflectometer—An alternative network analyzer," *IEEE Trans. Microwave Theory Tech.*, vol. MTT-25, pp. 1075–1083, Dec. 1977.

[9] F. M. Ghannouchi, R. G. Bosisio, and Y. Demers, "Load-pull characterization method using six-port techniques," in *Proc. IEEE I&M Technol. Conf.* (Washington, DC), Apr. 1989, pp. 536–539.

[10] F. M. Ghannouchi and R. G. Bosisio, "An alternative explicit six-port matrix calibration formalism using five standards," *IEEE Trans. Microwave Theory Tech.*, vol. 36, pp. 434–439, Mar. 1988.

[11] G. F. Engen and C. A. Hoer, "Thru-reflect line: An improved technique for calibrating the dual six-port automatic network analyzer," *IEEE Trans.*, vol. MTT-27, pp. 987–993, Dec. 1979.

[12] L. O. Chua and Y. W. Sing, "Non-linear lumped circuit model of GaAs MESFET," *IEEE Trans. Electron Devices*, vol. ED-30, p. 825, 1983.

[13] F. M. Ghannouchi, R. G. Bosisio, "A millimeter wave (18–40 GHz) coaxial and homodyne network analyzer," in *Proc. Conf. Precision Electromagnetic Measurements, CPEM 90* (Ottawa, Canada), June 11–14, 1990, pp. 55–56.

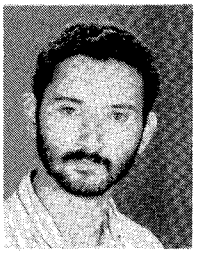

Fadhel M. Ghannouchi (S'84–M'88) received the degree in physics in 1980 from the University of Tunis. He then received the B.Eng. degree in engineering physics in 1983 and the M.Eng. and Ph.D. degrees in electrical engineering in 1984 and 1987, respectively, from Ecole Polytechnique de Montréal, Montreal, Canada.

He worked as a Lecturer during the period 1984–1986 at Ecole Polytechnique de Montréal, where he taught microwave theory and techniques. Since 1987, he has been a Senior Research Associate at the Microwave Research Laboratory of Ecole Polytechnique. Recently, he was appointed Assistant Professor with the same laboratory. Dr. Ghannouchi is a registered professional engineer in province of Quebec, Canada. His research interests are microwave/millimeter-wave metrology and CAD/CAM of microwave/millimeter-wave devices and circuits, with special emphasis on six-port measurement techniques and nonlinear circuits.

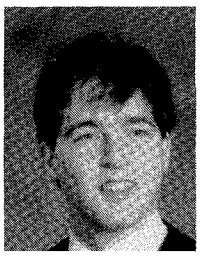

Robert Larose was born in Trois-Rivières, Canada, on December 20, 1964. He received the B.Ing. and M.Sc.A. degrees, both in electrical engineering, from École Polytechnique de Montréal, Canada, in 1988 and 1990 respectively. Since 1990 he has been with Centre d'Optique Photonique et Lasers, Québec, where he is pursuing the Ph.D. degree in electrical engineering. His work is concerned with nonlinear effects in optical fiber amplifiers and fiber lasers.

Renato G. Bosisio (M'79–SM'89) was born in Italy in 1930. He received the B.Sc. degree from McGill University, Montreal, Canada, in 1951, and the M.S.E.E. degree from the University of Florida, Gainesville, in 1963.

He has been engaged in microwave research and development work with various firms: Marconi and Varian in Canada, Sperry in the U.S., and English Electric in England. He is presently the Head of the Section d'Electromagnétisme et d'Hyperfréquences at Ecole Polytechnique de Montréal, Montreal, Canada, where he teaches microwave theory and techniques. He is actively engaged in six-port technology, dielectric measurements, and the computer-aided testing and design of both active and passive microwave devices.